A Collisional Radiative Model for Caesium and Its Application to an RF Source for Negative Hydrogen Ions

D. Wünderlich[1,a)], C. Wimmer[1)] and R. Friedl[2)]

[1]*Max-Planck-Institut für Plasmaphysik, Boltzmannstr. 2, 85748 Garching, Germany*
[2]*AG Experimentelle Plasmaphysik, Universität Augsburg, 86135 Augsburg, Germany*

[a)]Corresponding author: dirk.wuenderlich@ipp.mpg.de

Abstract. A collisional radiative (CR) model for caesium atoms in low-temperature, low-pressure hydrogen-caesium plasmas is introduced. This model includes the caesium ground state, 14 excited states, the singly charged caesium ion and the negative hydrogen ion. The reaction probabilities needed as input are based on data from the literature, using some scaling and extrapolations. Additionally, new cross sections for electron collision ionization and three-body recombination have been calculated. The relevance of mutual neutralization of positive caesium ions and negative hydrogen ions is highlighted: depending on the densities of the involved particle species, this excitation channel can have a significant influence on the population densities of excited states in the caesium atom. This strong influence is successfully verified by optical emission spectroscopy measurements performed at the IPP prototype negative hydrogen ion source for ITER NBI. As a consequence, population models for caesium in electronegative low-temperature, low-pressure hydrogen-caesium plasmas need to take into account the mutual neutralization process. The present CR model is an example for such models and represents an important prerequisite for deducing the total caesium density in surface production based negative hydrogen ion sources.

INTRODUCTION

Neutral beam injection (NBI) will be an integral part of the heating and current drive system of ITER. The heating beams (P=16.5 MW per beamline, two beamlines are presently envisaged) will deliver a beam energy of up to 1 MeV [1, 2] and hence the system has to be based on the production, extraction and acceleration of negative hydrogen or deuterium ions. Since 2007 the ITER baseline design for the NBI ion sources [1] is based on the RF driven prototype source with 1/8 area of the ITER source, developed at IPP Garching [3, 4]. The further development of this type of ion source towards application at ITER, taking place at IPP Garching and at Consorzio RFX Padua, follows an R&D roadmap defined by the European ITER domestic agency F4E [5].

Production of negative hydrogen (or deuterium) ions in such ion sources takes place mainly via the surface production process at the surface of the plasma grid (PG, the first grid of a multi-aperture, multi-grid extraction system): hydrogen atoms and positive ions approaching the PG surface are converted to negative ions by picking up electrons from the surface. The efficiency for this process depends inversely exponential on the surface work function. Thus, in order to increase the negative ion production rate, the work function of the PG surface is decreased by covering the grid with a caesium layer. Caesium is introduced to the ion source by an injection system containing a liquid [6] or solid [7] caesium reservoir. It is deposited at the inner surfaces of the ion source and is then released from these reservoirs and redistributed mainly by the influence of the low-temperature, low-pressure hydrogen plasma [8].

The thickness of the caesium layer (several monolayers) is significantly larger than the 0.6 ML for which an optimum work function (Φ=1.4 eV without the presence of impurities) would be expected [8]. Thus, the work function (a minimum of around 2.2 eV is achieved [9]; a value only slightly above the 2.14 eV for bulk caesium) is not a function of the layer thickness. Thus, for achieving and sustaining a low PG surface work function (one key issue in operating such negative hydrogen ion sources) it is not necessary to achieve a homogeneous caesium layer

thickness over the complete PG area and keep it constant in time. Instead, a caesium influx sufficient to counteract the degradation effects caused by the inclusion of impurities (from the plasma and the background gas) has to be provided: by covering a contaminated caesium layer with fresh caesium, the work function can be effectively reduced again [9, 10].

The caesium flux towards the PG cannot be measured directly, but it is correlated to the caesium density in the plasma volume close to the PG. One diagnostics method for determining this caesium density is optical emission spectroscopy (OES) [11]. In low-temperature, low-pressure hydrogen-caesium plasmas OES allows determining the population densities of some of the electronically excited states in the atom only (depending on the intensity of the emitted light and the sensitivity of the detector). For deducing the total caesium density (including besides the ground state all excited states and the ions), an appropriate population model has to be applied.

The simplest kind of population models are corona models – balancing electron collision excitation from the ground state with spontaneous emission. More sophisticated are collisional radiative (CR) models where all exciting and de-exciting processes relevant (i.e. with a non-negligible reaction rate) in the plasma under investigation are balanced. Up to now, no CR model was available for caesium in the low-temperature, low-pressure hydrogen-caesium plasma of negative hydrogen ion sources.

This paper describes a caesium CR model based on the flexible solver `Yacora` [12] and a new and comprehensive set of input data. The model is applied in order to validate for the plasmas under investigation the relevance of the mutual neutralization process of positive caesium ions and negative hydrogen ions, ending up in an excited caesium atom and a hydrogen atom in the ground state. In a second step, the high relevance for this process predicted by the model is experimentally demonstrated by applying the CR model to results of OES measurements at the IPP prototype source.

THE CR MODEL FOR CAESIUM

Physics of the CR model for caesium

CR models describe how the population densities of excited states in atoms or molecules depend on plasma parameters like the electron temperature T_e, the electron density n_e, the ground state density and the densities of all other particles involved in populating and depopulating the excited states [13, 14]. In order to do that, rate equations are solved which balance populating and de-populating channels for the excited states of the atom or molecule implemented in the model. These rate equations form a system of coupled ordinary differential equations. The solver `Yacora` – used for the investigations presented here – is based on an integrator for such equation systems.

Shown in figure 1 is an energy level diagram of caesium. The following 16 states included to the CR model for caesium in low-temperature, low-pressure hydrogen-caesium plasmas are indicated in green: the ground state 6^2S, all electronically excited states with an excitation energy $E_{ex}<3.3$ eV and orbital angular momentum quantum number $L\leq 2$ (i.e. up to the D states) and the singly charged ion Cs^+. Reason for taking into account also the ion is that the first ionization threshold for caesium atoms is low ($E_{Ion,I}=3.89$ eV). Thus, usually a large fraction of caesium is singly ionized in low-temperature, low-pressure hydrogen-caesium plasmas [15]. Due to this high ionization degree the reaction rate of recombining processes is high and the caesium ion has a high relevance for populating the excited states. The threshold for removing a second electron is comparatively high ($E_{Ion,II}=23.16$ eV) and hence, the doubly charged positive caesium ion can be neglected.

Indicated in Fig. 1 by arrows are the most probable optical transitions ($A_{ik}>10^4$ s^{-1}) in the wavelength range between 400 nm and 900 nm

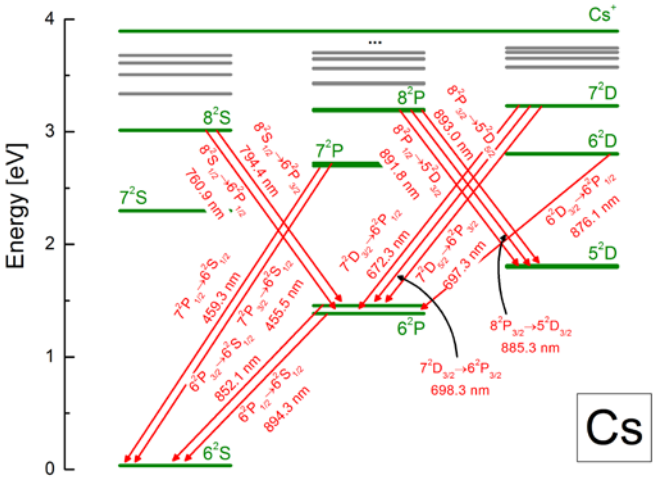

FIGURE 1. Energy level diagram of the caesium atom. Indicated (in green) are the states implemented to the CR model. Additionally shown are all optically allowed transitions between λ=400 nm and λ=900 nm and with $A_{ik}>10^4$ s^{-1} originating from these states.

originating from the excited states taken into account by the CR model. Among these are all transitions typically used for OES at caesium (the most prominent transition is the one at 852.1 nm).

The following reaction types are implemented within the CR model: spontaneous emission, electron collision excitation and de-excitation, electron collision ionization, three-body and radiative recombination of Cs^+ and mutual neutralization of Cs^+ with H^-. In order to enable implementing mutual neutralization, the list of states and species included in the model is extended by the negative hydrogen ion. Due to low reaction rates, no other heavy particle collisions besides mutual neutralization are taken into account by the CR model.

Due to low caesium ground state densities (lower as 10^{16} m^{-3}, [24]) resulting in a high mean free path of photons and additionally a low intensity of the photon field, processes like self-absorption due to optical thickness of emission lines [16] or photo ionization can be neglected.

The resulting rate equation for one excited state in the caesium atom is shown elsewhere [17].

Input parameters for the code are T_e, n_e and the densities of the ground state (6^2S) and the ions (Cs^+ and H^-). These densities are treated as quasi-constant during calculating the population densities of the excited states.

Probabilities for reactions interconnecting the energy levels of caesium

The 15 states of the caesium atom implemented within the CR model consist of nine electronic states, six of which (the states with orbital angular momentum quantum number $L \neq 0$) split up due to different total angular momentum quantum numbers J. While the reaction probabilities available in the literature for spontaneous emission cover all optically allowed transitions interconnecting these 15 states, almost all available cross sections for collisional processes neglect the fine-structure splitting.

Thus, the following procedure is implemented in the CR model: For collisional excitation and de-excitation as well as for ionization, recombination and mutual neutralization the fine structure is not taken into account. For example, during the electron collision excitation from 6^2S to 6^2P it is not distinguished between the two sub-states $6^2P_{1/2}$ and $6^2P_{3/2}$. The threshold energy of this excitation process is determined as the average energy of the sub-states. However, for determining the spontaneous emission rate the total population density of 6^2P is distributed among $6^2P_{1/2}$ (upper state of the line at 894.3 nm) and $6^2P_{3/2}$ (upper state of the line at 852.1 nm) according to the Boltzmann distribution defined by T_e. For these two sub-states then the appropriate transition probabilities are used. The choice of a Boltzmann distribution is justified by a high probability for electron collisions thermalizing the population densities of the sub-states resulting from the fine-structure splitting, caused by the very small energy difference between these states.

Output of the model are the calculated population densities for the nine implemented electronic states (i.e. neglecting the fine-structure splitting). These population densities can either be used directly or be split up subsequently (using again a Boltzmann distribution) in order to obtain the population densities of the sub-states caused by the fine-structure splitting. Either way, using the appropriate transition probabilities for spontaneous emission from and to the sub-states during the calculation process increases the accuracy of the modeling results compared to neglecting the fine-structure splitting.

The reaction probabilities (transition probabilities for spontaneous emission, cross sections for the collisional processes) for the different reaction types included in the model have been taken – as far as possible – from the literature. The cross sections for most of the collisional processes have been modified or extended in order to obtain a comprehensive set of all input data needed for the CR model. For electron collision ionization and three-body recombination new cross sections have been calculated using the Gryzinski [18] method and the Saha equation. The data from the literature as well as the performed modifications, extensions and calculations are described in detail elsewhere [17].

Dependence of population densities on the plasma parameters

Calculated population densities of the three excited states 6^2P, 7^2P and 7^2D are presented in this section. These are the upper states of seven of the most intense caesium emission lines (6^2P: at 852.1 nm and 894.3 nm, 7^2P: at 455.5 nm and 459.3 nm, 7^2D: at 672.3 nm, 697.3 nm and 698.3 nm, see also Fig. 1).

Without negative hydrogen ions ($n(H^-)=0$, i.e. mutual neutralization is switched off in the calculations), excitation by electron collision (mainly directly from the ground state 6^2S) is the dominant excitation channel in the plasmas under investigation. In this case, the dependence of the population densities on T_e is mainly determined by the well-known behavior of electron collision excitation rate coefficients: a strong increase for low T_e, followed by a

steady decrease of the gradient (Fig. 2a). This decrease of the gradient starts at a relatively low electron temperature ($T_e \approx 1.5 \ldots 2$ eV). Reason are the low threshold energies for direct electron collision excitation from the ground state. For high electron temperatures ($T_e > 20 \ldots 60$ eV, also depending on the electron density) the population densities decrease with the temperature (not shown here). For low electron densities ($n_e \leq 10^{16}$ m^{-3}) the calculated population densities approach the results of the corona models for the three states. The densities increase nearly linear with the electron density (Fig.2b). This is as well caused by the prevailing role of electron collisions for exciting the three states.

The negative hydrogen ion density in low-temperature, low-pressure hydrogen-caesium plasmas can reach values up to slightly above 10^{17} m^{-3} [19, 20, 21]. Population densities of 6^2P, 7^2P and 7^2D for negative hydrogen ion densities between 10^{14} m^{-3} and 10^{18} m^{-3} – calculated for typical parameters in such plasmas (T_e=2 eV, $n_e=10^{17}$ m^{-3} and $n(Cs^+)=9 \cdot n(Cs)$) – are shown in Fig. 3.

As can be expected, for low negative hydrogen ion densities the population densities approach the results for without negative ions. With increasing $n(H^-)$ a strong influence of mutual neutralization on the population densities of all three states is observed. Mutual neutralization can end up in an excited caesium atom in one of the following three states: 6^2P, 7^2S and 5^2D. Since 6^2P is one of these final states, its population density is directly increased with increasing $n(H^-)$. A slightly weaker increase of $n(7^2D)$ with $n(H^-)$ can be seen in the parameter range under investigation, while $n(7^2P)$ is much less affected. The increase of the two latter population densities is an indirect effect: first, the population densities of the three final states of mutual neutralization are increased. Then, these increased population densities are distributed among the other excited states by means of reactions interconnecting the excited states (mainly electron collisions and spontaneous emission). The additional excitation rate for 7^2P and 7^2D caused by these interconnecting reactions is roughly comparable. However, the reaction rate for electron collision excitation from the ground state (the main excitation channel in the case without H^-) is significantly smaller for 7^2D compared to 7^2P (caused by the higher excitation threshold energy). Consequently, the influence of the additional excitation caused by mutual neutralization on the total excitation rate of 7^2D is higher than for 7^2P.

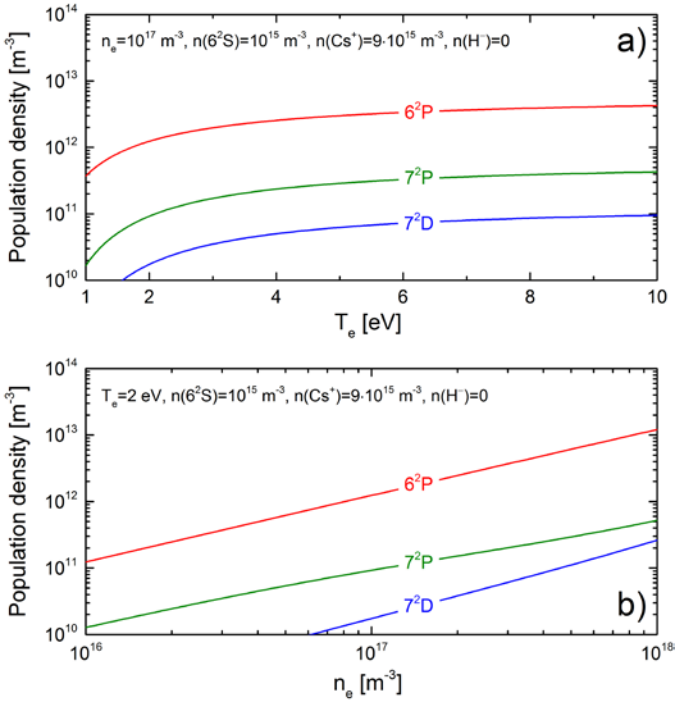

FIGURE 2. Population densities of the three states 6^2P, 7^2P and 7^2D in the caesium atom calculated using the CR model. a) Scan of the electron temperature T_e. b) Scan of the electron density n_e.

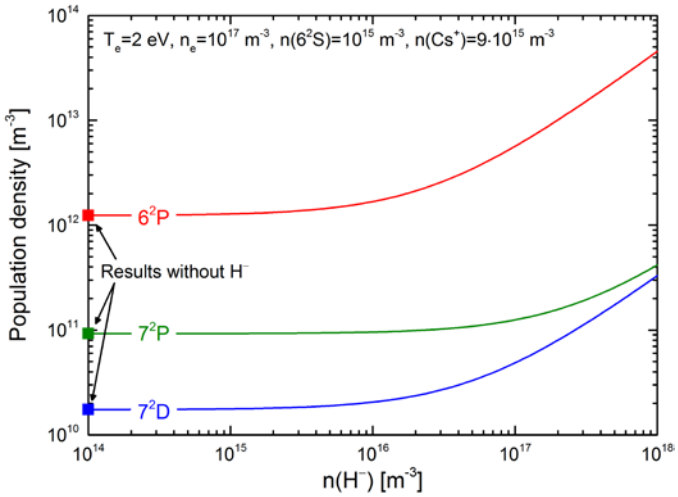

FIGURE 3. Population densities of the three states 6^2P, 7^2P and 7^2D in the caesium atom in dependence on the density of negative hydrogen ions (for $n(Cs^+) = 9 \cdot n(Cs)$).

A direct result of the increased excited state population densities is an increased intensity of the spontaneous emission lines originating from these states. Thus, OES is an appropriate tool to verify the strong influence of mutual neutralization predicted by the CR model.

COMPARISON WITH EXPERIMENTAL RESULTS

The experiment and the performed measurements

Population densities of excited caesium states calculated by the CR model are compared with OES results taken at the low-temperature, low-pressure plasma of the IPP prototype source at the BATMAN test facility [4].

A schematic view of the prototype source is shown in Fig. 4: the plasma is generated in a cylindrical driver by inductive RF coupling ($P_{RF,max}$≈100 kW). The plasma then expands into the expansion region where it is cooled (from T_e≥10 eV to ≈1 eV at n_e≈10^{17} m^{-3}) by means of a magnetic filter field (of some mT). The filter field is generated by rods of permanent magnets embedded into an external frame [22]. The dominant component of the filter field points into the horizontal direction. As already mentioned, the most important converter surface for generating negative hydrogen ions is the PG surface. The amount of co-extracted electrons, already reduced by the filter field, can be further decreased by a positive bias potential applied to the PG with respect to the source body extended by a so-called bias plate. The caesium injection system is attached to the upper part of the source back plate.

For the performed investigations two diagnostic ports are used for OES providing horizontal lines of sight (LOS) parallel to the PG with 2.0 cm distance to the grid: one (XR1) in the upper part of the ion source and another (XL1) in the lower part (see Fig. 4). Reason for using two different horizontal LOS is that during previous campaigns strong vertical non-uniformities of the plasma in front of the extraction system have been observed, caused by plasma drifts [4]. These drifts are induced by the horizontal filter field in interplay with axial potential gradients in the plasma. During the present measurements the magnetic field was used in the configuration "drift up", i.e. close to the PG a vertical shift of the bulk plasma towards the upper half of the ion source takes place.

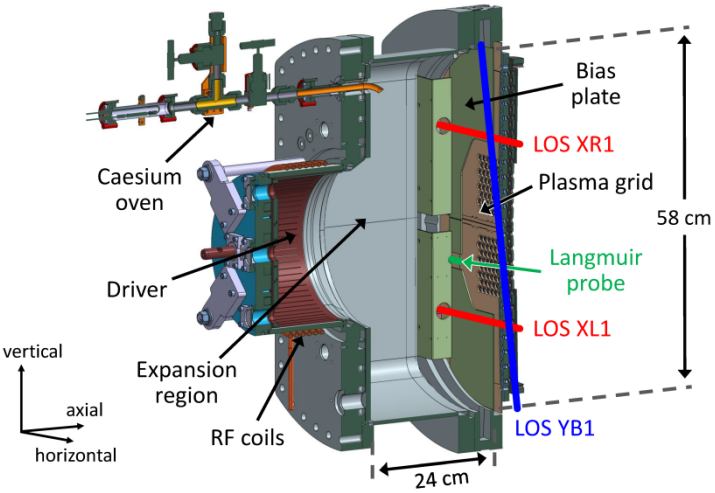

FIGURE 4. Schematic view of the IPP prototype negative hydrogen ion source including the two horizontal lines of sight (XR1 and XL1) used for the performed OES measurements, the vertical line of sight (YB1) of the laser absorption spectroscopy and one of the two Langmuir probes.

The intensity per unit volume of six emission lines originating from the excited states 6^2P, 7^2P and 7^2D along these two LOS was determined by means of an absolutely calibrated spectrometer (ACTON SpectraPro-750i). The error bar of these measurements is smaller than 10 %. The LOS averaged population densities of the three excited states were deduced by dividing the measured line emissivities by the according Einstein coefficient and summing up – for each of the three states – the results for the two respective sub-states resulting from the fine-structure splitting.

In order to check the predicted high relevance of mutual neutralization, these measured population densities are compared with results of the CR model. For each of the two LOS measurements for two different plasma regimes were performed: firstly, the PG bias was set to the floating potential ("without bias"). And secondly, the PG bias was optimized for reducing the co-extracted electron current without affecting too much the extracted negative ion current ("with bias"). The PG bias influences mainly the absolute value of the plasma density close to the PG and the effect of the vertical plasma drift, the latter being directly correlated to the plasma distribution.

A prerequisite of performing CR model calculations is the knowledge of the plasma parameters (T_e, n_e, $n(6^2S)$, $n(Cs^+)$, $n(H^-)$) in the discharges under investigation. An overview of the plasma parameters used as input for the model is given in the following section.

Plasma parameters in the IPP prototype source

During the investigated discharges the local electron temperature and electron density have been determined by two Langmuir probes [23]. These probes are positioned at the vertical side walls of the ion source – one probe in the

upper part of the source and the second in the lower part. The axial distance between the probe tips and the PG (Δ_{axial}=0.8 cm) and also the vertical distance from the center of the PG is smaller compared to the LOS used for OES – as can be seen in Fig. 4. Shown in the figure is only one of the probes (in the lower part of the source), another one is located in the upper part of the ion source close to the side wall cut away in the figure. The electron temperature was determined by the probes to be 2.0 eV with bias and 2.1 eV without bias. The measured electron densities are between $2.8 \cdot 10^{16}$ m^{-3} and 10^{17} m^{-3} where n_e is always higher in the upper part of the source compared to the lower part. Without bias the ratio $n_{e,\ upper}/n_{e,\ lower}$ is 2.1 and it increases to 3.6 with bias. These observations can be explained by the influence of the PG bias on the upward vertical plasma drift mentioned before.

For the caesium ground state density $n(6^2S)$ a lower limit between $6 \cdot 10^{14}$ m^{-3} and $7 \cdot 10^{14}$ m^{-3} has been determined during the present campaign by laser absorption spectroscopy [24] along a vertical LOS (YB1, see Fig. 4). These caesium densities are not directly comparable to the OES and CR model results since the vertical LOS averages – in contrast to the two horizontal LOS used for OES – the caesium densities in the upper and the lower part of the ion source. Laser absorption spectroscopy measurements based on the two LOS XR1 and XL1 performed during previous experimental campaigns indicate that due to the position of the caesium injection system (at the upper part of the source back plate) the caesium density in the upper part of the ion source usually is larger compared to the lower part. Typical values for the ratio $n(6^2S)_{upper}/n(6^2S)_{lower}$ determined by laser absorption spectroscopy during plasma pulses are between one and two. Depending on the caesium distribution as well as the direction and the strength of the vertical plasma drift sometimes also significantly higher values of this ratio are possible.

The other input parameters for the CR model have not been determined during the present experimental campaign, but typical values from previous measurements are used: by OES the ionization degree of caesium has been determined to be around 90 % [15]. The density $n(H^-)$ of negative hydrogen ions close to the PG is taken from laser detachment [19] and cavity ring-down [20, 21] measurements: depending on the filling pressure, the applied RF power and the status of the caesium conditioning, $n(H^-)$ can reach values slightly higher than 10^{17} m^{-3}. No measured upper/lower ratio of the negative ion density is available.

The described plasma parameters are used as starting point for an optimization procedure: for T_e and n_e deviations of up to ±1 eV and ±15 % from the measured values were allowed, respectively (representing the error bar of the probe results). The caesium ground state density $n(6^2S)$ and $n(H^-)$ are free parameters. The ratio of singly ionized caesium to caesium in its ground state is set to the fixed value 9.0.

Results of applying the CR model for calculating population densities

The population densities of the states 6^2P, 7^2P and 7^2D from OES for the four performed measurements are shown in Fig. 5 (in full symbols). The results of the performed CR model calculations are shown in open squares. The input parameters used for these calculations are summarized in table 1. Taking mutual neutralization into account, for all measurements a good agreement between the population densities measured by OES and the CR model results is obtained.

The predicted influence of mutual neutralization on the population densities can clearly be seen: besides the best possible match of model to experiment Fig. 5 additionally shows (open circles) the result for the same set of input parameters, but calculated without mutual neutralization. While for the upper LOS (XR1) a good match of CR model results and measurements is possible with and without mutual neutralization, for the lower LOS (XL1) mutual neutralization is necessary for obtaining a good agreement. The enhancement caused by mutual neutralization is particularly pronounced

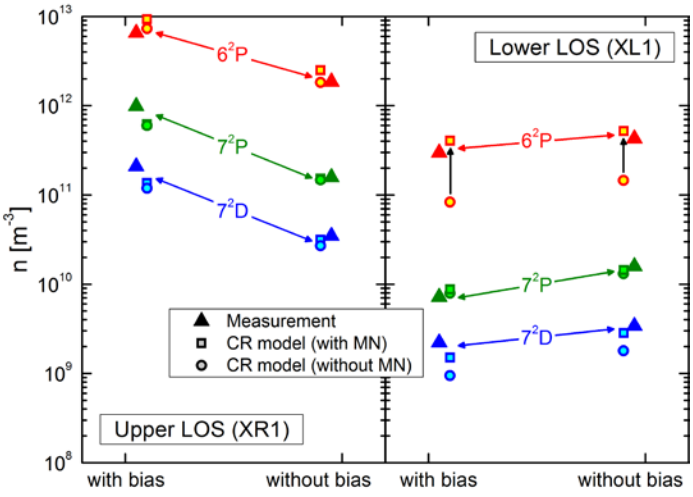

FIGURE 5. Comparison of experimentally determined population densities for the four performed measurements (full triangles) and CR model results with (open squares) and without mutual neutralization (open circles). The strong influence of mutual neutralization on the population density of $n(6^2P)$ is indicated by vertical arrows.

for 6^2P (indicated in Fig. 5 by vertical arrows): compared to the measurements the population densities from the CR model without mutual neutralization are too small by a factor of 3–3.5. The effect of mutual neutralization is weaker for 7^2D and negligible for 7^2P. This sequence fits very well to the results shown in Fig. 3.

TABLE 1. Plasma parameters used in order to reproduce the measured population densities by the CR model.

Measurement set	T_e [eV]	n_e [m^{-3}]	$n(6^2S)$ [m^{-3}]	$n(H^-)$ [m^{-3}]
XR1, with bias	2.5	$1.0 \cdot 10^{17}$	$4.5 \cdot 10^{15}$	$1.0 \cdot 10^{16}$
XR1, without bias	2.2	$8.7 \cdot 10^{16}$	$1.5 \cdot 10^{15}$	$1.0 \cdot 10^{16}$
XL1, with bias	2.0	$2.8 \cdot 10^{16}$	$2.4 \cdot 10^{14}$	$3.0 \cdot 10^{16}$
XL1, without bias	2.0	$4.2 \cdot 10^{16}$	$2.8 \cdot 10^{14}$	$3.0 \cdot 10^{16}$

The electron temperatures used as input for the calculations are well within the error bar of the Langmuir probe results. The electron densities from the probe measurements could be used directly as model input. This very good agreement is somewhat surprising since – as described above – the position of the probes is different from the LOS used for OES. Additionally the probes determine the local plasma parameters close to the side walls while the OES results are averaged along the LOS.

The caesium ground state densities determined by the CR model have the same order of magnitude as the results of laser absorption spectroscopy. This agreement is quite good taking into account the different geometries of the LOS used for OES and laser absorption spectroscopy, discussed in the previous section. The caesium ground state density along the upper LOS from the model is by a factor of 6.2 (without bias) or 18.7 (with bias) larger compared to the lower LOS. This upper/lower asymmetry of $n(6^2S)$ is higher than the typical asymmetry factors observed previously by laser absorption but smaller compared to the maximum measured values.

The negative hydrogen ion densities from the CR model (10^{16} m^{-3} for the upper LOS and $3 \cdot 10^{16}$ m^{-3} for the lower LOS) are in general agreement with the results of the laser detachment and cavity ring-down measurements based on different LOS. The value 10^{16} m^{-3} for $n(H^-)$ along the upper LOS represents an upper limit since – as can be seen in Fig. 5 – the influence of mutual neutralization on the population densities is almost negligible.

The much stronger influence of mutual neutralization on the population densities along the lower LOS (XL1) is caused by an asymmetry in the plasma parameters (an effect of the plasma drift): direct excitation from the ground state $n(6^2S)$ is the dominant excitation channel for the upper LOS (XR1). Along the lower LOS (XL1) n_e is smaller and $n(H^-)$ is higher, resulting in a non-negligible relevance of the mutual neutralization channel.

Concluding, it is possible for all performed measurements to match the caesium population densities calculated by the CR model to the OES results. If the mutual neutralization process is taken into account the input parameters used by the CR model agree well with measurements performed in parallel with the OES measurements or during previous experimental campaigns. The CR model for caesium in low-temperature, low-pressure hydrogen-caesium plasmas of surface production based negative hydrogen ion sources can be used in a next step – for example – to determine the density of the singly charged positive caesium ion from measured line intensities (for known negative hydrogen ion density). Due to the high ionization degree of caesium precise knowledge of $n(Cs^+)$ is an important prerequisite for determining total caesium densities.

As already shown, the increased population densities of the final states of the mutual neutralization process are distributed among the other excited states by means of interconnecting reactions. Thus, only CR models are suited to predict for all excited states the equilibrium resulting from these re-distribution processes. Corona models (taking into account the direct excitation channel only) are not sufficient to describe the population densities of the excited states of the caesium atom. However, a corona model extended by the mutual neutralization process can be applied to determine the population density of a single excited state if the influence of re-distributing the population densities of the excited states is small.

SUMMARY

Based on the flexible solver `Yacora` a CR model for the caesium atom was constructed. This model focusses on caesium in the low-temperature, low-pressure hydrogen-caesium plasmas of surface production based negative hydrogen ion sources, as for example currently being in development for NBI at ITER.

The most interesting reaction included in the model is mutual neutralization of positive caesium ions and negative hydrogen ions: depending on the densities of the two involved particle species this process can significantly enhance the population of several excited states in the caesium atom and thus also the intensity of the emission lines originating from these excited states. In order to test this prediction, OES measurements were performed at the IPP prototype source for negative hydrogen ions.

A very good agreement of the CR model results with the population densities determined by OES could be obtained for two different LOS and in two different plasma regimes. The plasma parameters used as input for the CR model agree well with results from other diagnostic techniques.

These results verify the predicted high relevance of mutual neutralization and point out that population models for caesium in the electronegative plasma of the boundary layer in negative ion sources based on surface conversion (i.e. in plasmas with a high density of H^-) need to take into account the mutual neutralization process. Depending on the field of application such models can either be an extended corona model or the present CR model. Since the latter takes into account several excited states and additionally the caesium ion, it represents an important prerequisite for deducing the total caesium density (including the population densities of the excited states and the density of the ion). Thus, the CR model might be – for example – extremely useful for supporting the caesium conditioning process with the aim to obtain high and stable extracted values of the extracted negative ion current.

ACKNOWLEDGMENTS

This work has been carried out within the framework of the EUROfusion Consortium and has received funding from the European Union's Horizon 2020 research and innovation programme under grant agreement number 633053. The views and opinions expressed herein do not necessarily reflect those of the European Commission.

The work was supported by a grant from Fusion for Energy (F4E-2008-GRT-007) under the responsibility of Antonio Masiello. The opinions expressed herein are those of the authors only and do not represent the Fusion for Energys official position.

REFERENCES

1. R. Hemsworth, A. Tanga and V. Antoni, Rev. Sci. Instrum. 79, 02C109, 2008.
2. R. Hemsworth et al, Nucl. Fusion 49, 045006, 2009
3. E. Speth et al, Nucl. Fusion 46, S220, 2006
4. U. Fantz et al, Rev. Sci. Instrum. 79, 02A511, 2008.
5. A. Masiello et al, Fusion Eng. Des. 84, 1276, 2009.
6. M. Fröschle et al, Fusion Eng. Des. 84, 788, 2009.
7. U. Fantz, R. Friedl and M. Fröschle, Rev. Sci. Instrum. 83, 123305, 2012.
8. R. Gutser et al, Plasma Phys. Control. Fusion 53, 105014, 2011.
9. R. Gutser, C. Wimmer and U. Fantz, Rev. Sci. Instrum. 82, 023506, 2011.
10. R. Friedl and U. Fantz, *Contribution to this conference*
11. U. Fantz et al, Nucl Fusion 46, S297, 2006.
12. D. Wünderlich, S. Dietrich and U. Fantz, J. Quant. Spectrosc. Radiat. Transfer. 110, 62, 2009.
13. D. R. Bates, A. E. Kingston and R. W. P. McWirter, Proc. R. Soc. Lond. A 267, 297, 1962.
14. T. Fujimoto, J. Quant. Spectrosc. Radiat. Transfer 21, 439, 1979.
15. U. Fantz et al, Fusion Eng. Des. 74, 299, 2005.
16. K. Behringer and U. Fantz, New. J. Phys. 2, 23, 2000.
17. D. Wünderlich, C. Wimmer and R. Friedl, J. Quant. Spectrosc. Radiat. Transfer. 149, 360, 2014.
18. M. Gryzinski, Phys. Rev. 138, A336, 1965.
19. S. Christ–Koch et al, Plasma Sources Sci. Technol. 18, 025003, 2009.
20. M. Berger et al, Plasma Sources Sci. Technol. 18, 025004, 2009.
21. C. Wimmer, U. Fantz and the NNBI–Team, AIP Conf. Proc. 1515, 246, 2013.
22. P. Franzen et al, Plasma Phys. Control. Fusion 53, 115006, 2011.
23. L. Schiesko, Plasma Phys. Control. Fusion 54, 105002, 2012.
24. U. Fantz and C. Wimmer, J. Phys. D 44, 335202, 2011.